Available online at www.sciencedirect.com
SCIENCE DIRECT®
Journal of Computational Physics 214 (2006) 299–315
JOURNAL OF COMPUTATIONAL PHYSICS
www.elsevier.com/locate/jcp

On the integration of equations of motion for particle-in-cell codes ☆

V. Fuchs [a,*], J.P. Gunn [b]

[a] *Institute of Plasma Physics, Czech Academy of Sciences, Tokamak, Association EURATOM/IPP.CR, Za Slovankou 3, 18200 Praha 8, 18200 Prague, Czech Republic*
[b] *Association EURATOM-CEA/DSM/DRFC, Centre de Cadarache, 13108 St. Paul Lez Durance, France*

Received 25 May 2005; received in revised form 31 August 2005; accepted 16 September 2005
Available online 21 November 2005

Abstract

An area-preserving implementation of the 2nd order Runge–Kutta integration method for equations of motion is presented. For forces independent of velocity the scheme possesses the same numerical simplicity and stability as the leapfrog method, and is not implicit for forces which do depend on velocity. It can be therefore easily applied where the leapfrog method in general cannot. We discuss the stability of the new scheme and test its performance in calculations of particle motion in three cases of interest. First, in the ubiquitous and numerically demanding example of nonlinear interaction of particles with a propagating plane wave, second, in the case of particle motion in a static magnetic field and, third, in a nonlinear dissipative case leading to a limit cycle. We compare computed orbits with exact orbits and with results from the leapfrog and other low-order integration schemes. Of special interest is the role of intrinsic stochasticity introduced by time differencing, which can destroy orbits of an otherwise exactly integrable system and therefore constitutes a restriction on the applicability of an integration scheme in such a context [A. Friedman, S.P. Auerbach, J. Comput. Phys. 93 (1991) 171]. In particular, we show that for a plane wave the new scheme proposed herein can be reduced to a symmetric standard map. This leads to the nonlinear stability condition $\Delta t\,\omega_B \leqslant 1$, where Δt is the time step and ω_B the particle bounce frequency.

PACS: 52.65.Cc; 52.65.Rr; 52.35.Mw

Keywords: Equations of motion; 2nd Order integration methods; Nonlinear oscillations

1. Introduction

An essential ingredient of non-relativistic, electrostatic particle-in-cell (PIC) codes with many particles and evolving on long time scales is a sufficiently simple, accurate and stable integration scheme for the electron and ion equations of motion

☆ Work partly supported by the Czech Republic Grant Project GACR 202/04/0360.
* Corresponding author. Tel.: +420 266053168; fax: +420 286586389.
E-mail address: fuchs@ipp.cas.cz (V. Fuchs).

0021-9991/$ - see front matter
doi:10.1016/j.jcp.2005.09.026

$$\mathrm{d}v_{\mathrm{e,i}}/\mathrm{d}t \equiv \dot{v}_{\mathrm{e,i}} = qE_z/m + F_{\mathrm{e,i}}, \quad \mathrm{d}z/\mathrm{d}t \equiv \dot{z} = v, \tag{1}$$

where E_Z is the self-consistent electric field, $F_{\mathrm{e,i}}$ are the external forces and q/m is the particle charge to mass ratio. An integration scheme having the desired properties is the well-known time-centered leapfrog (LF) method [1]

$$v_{n+1/2} - v_{n-1/2} = \Delta t\, a_n, \quad z_{n+1} - z_n = \Delta t\, v_{n+1/2} \tag{2}$$

accurate to 2nd order with respect to the time-step Δt, and implicit when the acceleration a_n depends on velocity. The subscripts in (2) indicate time-levels. An implicit implementation is straightforward only in exceptionally simple cases, such as, e.g., the case of the Lorentz force (see Section 4) or of linear damping, by taking $v_n = (v_{n+1/2} + v_{n-1/2})/2$. However, such a treatment is computationally very demanding, possibly prohibitive, for more complicated situations of interest such as dissipative systems or in Monte-Carlo treatments of particle collisions [2] and/or interactions of particles with radio-frequency fields [3]. Another limitation which owes to the half time-step shift between position and velocity in the LF method is the need for a constant time step during the integration process.

In this paper, we look for a viable time-aligned alternative to the LF method. We concentrate on the 2nd order accurate Runge–Kutta (RK) method [4,5] which appears promising, since time-centering in the method is approximately achieved by anticipating an average force acting between two successive time steps. For equations of motion the usual 2nd order RK algorithm gives

$$\begin{aligned} &v_{n+1} - v_n = \frac{\Delta t}{2}(a_n + a^*_{n+1}), \quad z_{n+1} - z_n = \frac{\Delta t}{2}(v_n + v^*_{n+1}),\\ &a_n = a(t_n, v_n, z_n), \quad a^*_{n+1} = a(t_n + \Delta t, v_n + \Delta t\, a_n, z_n + \Delta t\, v_n),\\ &v^*_{n+1} = v_n + \Delta t\, a_n. \end{aligned} \tag{3}$$

The scheme is explicit and requires two evaluations of the applied force, one at $t = t_n$ and one at $t = t_n + \Delta t$. The scheme is clearly only as good as the approximation for a^*_{n+1}. We will therefore also consider the midpoint Runge–Kutta scheme [5], which, in general, also requires two evaluations of the force per time-step, one at t_n and the other at the mid-point $t_n + \Delta t/2$:

$$\begin{aligned} &t_m = t_n + \Delta t/2, \quad v_m = v_n + a_n \Delta t/2, \quad z_m = z_n + v_n \Delta t/2,\\ &a_n = a(t_n, v_n, z_n), \quad a_m = a(t_m, v_m, z_m),\\ &v_{n+1} - v_n = \Delta t\, a_m, \quad z_{n+1} - z_n = \Delta t\, v_m. \end{aligned} \tag{4}$$

We will show here that an area-preserving combination of the two methods (3) and (4) is not less stable than the LF method in the presence of linear and nonlinear oscillations. While the linear stability of time-differenced integration schemes is well-understood as being related to normal modes which are not modes of the exact equation [6–9], the application of the LF method to nonlinear oscillations was shown by Friedman and Auerbach [10] and Auerbach and Friedman [11] to be limited beyond a certain threshold by "numerical stochasticity", which arises from time differencing rather than from any intervening physical process. Auerbach and Friedman [11] also demonstrate the connection between area preservation and long term stability of the computed orbits. Following the Hamiltonian spirit of [10,11], we emphasize here the analogy between a 2nd order time-differencing scheme for an equation of motion and a mapping of phase space (v, z) onto itself. The analogy is useful in as much as the mapping represents a perturbation of an originally integrable Hamiltonian. Thus, area-preservation of the associated time-differencing scheme is essential for a number of related reasons [12]. First, the integration scheme should preserve constants of motion and make them apparent in the surface of section. Second, we show here that area-preservation is necessary for (at least conditional) numerical linear stability of the differencing scheme. Since the time differencing constitutes a perturbation of an integrable Hamiltonian, the surface of section will reveal the destruction of regular particle orbits caused by the time differencing, rather than by perturbations of physical origin. The applicability of a particular integration method to nonlinear oscillations is therefore limited by the associated stochasticity threshold.

We will discuss the stability and numerically test the performance of the new integration scheme proposed herein (Eq. (13) of the next section) by comparing particle orbits with results from other schemes and mainly with exact and LF-produced reference results. For the tests we selected three familiar problems of interest. The

first is particle motion in a propagating plane wave. The second is the four-dimensional case of particle motion in a static magnetic field where the force depends on velocities, and for which the LF method has a simple implicit solution. This case is interesting because the higher (than two) dimensionality allows more than one implementation of a particular integration scheme. Also, the velocity space gyro-orbit is mathematically equivalent to the harmonic oscillator. Both above cases are conservative and the equations have an exact solution. The third test case is the non-conservative case of a harmonic oscillator perturbed by a nonlinear dissipative term, such as the van der Pol oscillator [13], leading to stable motion on a limit cycle.

Given the central role occupied by equations of motion in PIC codes, the problem of finding a suitable integration scheme has in the past received considerable attention ([6–9] and references therein). Along with the effort of developing suitable schemes, methods for the analysis of their numerical stability were developed by Langdon [6], Cohen et al. [7], and Hockney and Eastwood [9]. Numerical amplitude instability and phase shift can arise in finite difference schemes even for an inherently stable equation because of normal modes which are not solutions of the exact equation [6–9]. The approach in [6,7] is based upon a class of integration schemes which differ from the leapfrog scheme by the possible effect of the acting force at past time levels, a_{n-1}, a_{n-2} etc. If a_{n+1} is also involved then the scheme is implicit. The dispersion relation and stability conditions for this particular class of schemes was derived in [6,7] for the linear harmonic oscillator force $a = -z\omega_0^2$. The method is reviewed, together with a discussion of a number of specific integration schemes, in Birdsall and Langdon [8]. By contrast, Hockney and Eastwood [9] discuss stability with respect to round-off errors, i.e., with respect to perturbations ε of particle velocity and position, for a force of arbitrary form. In the Hockney and Eastwood method, the integration scheme time-difference equations are expanded around the round-off error-free quantities to 1st order in ε which produces the transfer matrix relating successive time levels of the perturbation evolution. Eigenvalues of the transfer matrix determine the stability properties and the eigenvalue equation is equivalent to the dispersion relation.

The present analysis of integration schemes begins with the discussion of linear stability using the methods quoted above. This is followed by the analysis of nonlinear stability, specifically of the intrinsic stochasticity associated with the time differencing of electron interaction with a plane wave. This leads to a numerical stability criterion for integrating the nonlinear oscillator. We view an integration scheme as an iterated map in phase space (v, z) and exploit some useful properties of such maps, particularly the area-preservation property expressed quantitatively by its Jacobian [12]. In particular, area preservation of a non-implicit integration scheme should be expected for a conserved Hamiltonian, i.e., in the absence of damping or amplification in the system. This is not necessarily true for implicit schemes [10]. Further for non-implicit schemes, we shall also see that if $J > 1$ then the integration scheme is numerically unconditionally unstable and that $J = 1$ is a necessary condition for numerical stability. The standard RK schemes (3) and (4) are never area preserving and thus are numerically unconditionally unstable. However, conditional stability can be attained by an implementation which preserves phase space area.

For numerical testing of the various schemes under consideration here we choose, at an advantage, closed orbit solutions. The first two cases, trapped electron orbits in a non-linear wave and orbits in a static magnetic field, are exactly integrable. In the first case the motion has a first integral in the wave reference frame so that the long-term stability of computed trapped orbits is easily assessed on comparison with the exact orbit. Furthermore, the collapse of orbits due to intrinsic stochasticity is conveniently visualized in Poincare surface of section plots. The second example brings to light certain specific aspects of multi-dimensional systems, such as more freedom in the choice of an appropriate implementation. In our third test case – of the nonlinearly perturbed harmonic oscillator – the orbit winds up onto a stable limit cycle which again is a convenient reference orbit for comparison with the computed solution.

In Section 2, we discuss numerical stability and accuracy and in Section 3, we discuss numerical integration in the nonlinear case of a periodic force. In Section 4, we consider integration in the presence of a static magnetic field and of nonlinear dissipation. Finally, in Section 5, we give our conclusions.

2. Stability and accuracy of 2nd order Runge–Kutta integration schemes

As discussed in detail in [8], the self-consistent electric field E_Z is only a function of time and particle position. If, in addition, the external forces $a_{e,i}$ acting on the particles are also independent of velocity, then the

leapfrog method (2) can be used for explicitly integrating the equations of motion (1). The LF method is 2nd order accurate and manifestly time-centered. Furthermore, the mapping (2) is area preserving, quantitatively expressed by a unity Jacobian:

$$J = \det\begin{pmatrix} \partial v_{n+\frac{1}{2}}/\partial v_{n-\frac{1}{2}} & \partial v_{n+\frac{1}{2}}/\partial z_{n-1} \\ \partial z_{n+1}/\partial v_{n-\frac{1}{2}} & \partial z_{n+1}/\partial z_{n-1} \end{pmatrix} = \det\begin{pmatrix} 1 & \Delta t\,\partial a_n/\partial z \\ \Delta t & 1+\Delta t^2\,\partial a_n/\partial z \end{pmatrix} = 1. \tag{5}$$

In Section 2.1, we will show that area preservation is a necessary but not sufficient stability condition. For example, the stability condition for the LF scheme is [9]

$$0 \leqslant -\Gamma \leqslant 2, \quad \Gamma = (\partial a/\partial z)(\Delta t^2/2). \tag{6}$$

For the linear oscillator $a = -\omega_0^2 z$ the condition (6) implies $\omega_0 \Delta t \leqslant 2$, in agreement with previous results [5,6]. It is interesting to evaluate the leapfrog Jacobian for a velocity-dependent force $a = a(t_n, v_n, z_n)$. Approximating v_n by the average $v_n = (v_{n+1/2} + v_{n-1/2})/2$ gives

$$J_{\mathrm{LF}} = \frac{1+\frac{\Delta t}{2}\frac{\partial a}{\partial v}}{1-\frac{\Delta t}{2}\frac{\partial a}{\partial v}}. \tag{7}$$

As expected, area is not preserved in this case. Iterations of an implicit scheme are computationally too demanding in most situations of interest but for linear damping where the force is given by $a = a(t,z) - vv$ the leapfrog scheme takes the form

$$v_{n+1/2} - v_{n-1/2}\frac{1-v\Delta t/2}{1+v\Delta t/2} = \frac{\Delta t\, a(t_n, z_n)}{1+v\Delta t/2}, \quad z_{n+1} - z_n = \Delta t\, v_{n+1/2} \tag{8}$$

which could be used for a reference calculation. The solution naturally tends to either a stable focal point or it diverges, depending respectively on the sign of v. Therefore, in Section 4 we instead deal with velocity dependent systems which exhibit easy-to-monitor finite-size stable orbits. First, we deal with the four-dimensional velocity-dependent magnetic field interaction which conserves energy, and then with the perturbed harmonic oscillator whose solution tends to a stable limit cycle.

Having previously emphasized that an integration scheme for a Hamiltonian system should preserve area, our principal task now is to identify such an integration scheme which unlike the leapfrog scheme is not implicit for forces dependent on velocity. Let us therefore consider the 2nd order Runge–Kutta (RK) schemes (3) and (4). These two basic schemes are never area preserving. For example, the Jacobian of the transformation (3) is

$$J_{\mathrm{RK}} = 1 + \frac{\Delta t}{2}\left(\frac{\partial a}{\partial v} + \frac{\partial a^*}{\partial v}\right) + \frac{(\Delta t)^3}{4}\left(\frac{\partial a}{\partial z}\frac{\partial a^*}{\partial v} - \frac{\partial a}{\partial v}\frac{\partial a^*}{\partial z}\right) + \frac{(\Delta t)^4}{4}\frac{\partial a}{\partial z}\frac{\partial a^*}{\partial z}. \tag{9}$$

If the force does not depend on velocity, then to 4th order in Δt

$$J_{\mathrm{RK}} = 1 + \frac{(\Delta t)^4}{4}\left(\frac{\partial a}{\partial z}\right)^2 + \mathrm{O}(\Delta t^5). \tag{10}$$

Hence, $J_{\mathrm{RK}} > 1$ to leading order in Δt. This, as we shall see below, implies unconditional numerical instability with respect to perturbations of the solution.

We now find it useful to introduce the concept of semi-implicitness. In a mapping of phase space $\vec{w} = (\vec{v}, \vec{z})$ onto itself, each component w_α can in general be given as a function of both the old (nth time level) and the new components, i.e., $\vec{w}_{n+1} = f_w(\vec{w}_n, \vec{w}_{n+1})$. Such a mapping is termed explicit if the transformation functions f_w do not depend on new components $\vec{w}_{n+1}$ and is termed implicit if at least for one of the components, $\partial f_{w_\alpha}/\partial w_{\alpha,n+1} \neq 0$. We term a mapping semi-implicit if for all components $\partial f_{w_\alpha}/\partial w_{\alpha,n+1} = 0$ but for at least one component, $\partial f_{w_\alpha}/\partial w_{\beta,n+1} \neq 0, \alpha \neq \beta$. By this definition the LF mapping (2) is semi-implicit while the RK mappings (3) and (4) are explicit.

The schemes (3) and (4) can be immediately substantially improved, without any extra effort, by a semi-implicit implementation. In the two-dimensional case this is trivially achieved by using the calculated velocity v_{n+1} in the position equation instead of the 1st order correction anticipated by the RK method. The Jacobian can be then generally expressed in the form

$$J = \frac{\partial v_{n+1}}{\partial v_n} - \frac{\Delta t}{2}\frac{\partial v_{n+1}}{\partial z_n}. \tag{11}$$

For scheme (3) this gives

$$J_{\mathrm{RK}} = 1 + \frac{\Delta t}{2}\left(\frac{\partial a}{\partial v} + \frac{\partial a^*}{\partial v}\right) + \frac{(\Delta t)^4}{4}\left(\frac{\partial a^*}{\partial z} - \frac{\partial a}{\partial z}\right). \tag{12}$$

We now see that the involvement of the force at two different times, $a(t)$ and $a^*(t+\Delta t)$ still destroys area preservation, even when the force is not velocity-dependent. We therefore next introduce a modification of Eq. (4) that is semi-implicit through the evaluation of $z_{n+1} - z_n$ depending on an average of v_n and v_{n+1} rather than the extrapolation v_m, such that Eq. (4) become:

$$\begin{aligned} &t_m = t_n + \Delta t/2, \quad v_m = v_n + a_n\Delta t/2, \quad z_m = z_n + v_n\Delta t/2,\\ &a_n = a(t_n, v_n, z_n), \quad a_m = a(t_m, v_m, z_m),\\ &v_{n+1} - v_n = \Delta t\, a_m, \quad z_{n+1} - z_n = \Delta t\,(v_n + v_{n+1})/2 \end{aligned} \tag{13}$$

The Jacobian (11) of the mapping (13) is

$$J_{\mathrm{SIMP}} = 1 + \Delta t\frac{\partial a_m}{\partial v} \tag{14}$$

to be compared with J_{LF}, Eq. (7). In both cases $J = 1$ for a velocity independent force. Another important distinction between (13) and the standard midpoint scheme (4) is that for a force independent of velocity only one evaluation of the force is needed in (13). Henceforth, we refer to the scheme (13) as SIMP (semi-implicit midpoint). We now turn to the analysis of linear stability of the preceding schemes.

2.1. Linear stability

We begin with applying the stability analysis method of Langdon [7] and Cohen et al. [8], who proposed and studied in detail the class of integration schemes

$$\frac{z_{n+1} - 2z_n + z_{n-1}}{(\Delta t)^2} = a_n + c_0(a_{n+1} - 2a_n + a_{n-1}) + c_1(a_n - 2a_{n-1} + a_{n-2}) + c_2(a_{n-1} - 2a_{n-2} + a_{n-3}) + \cdots. \tag{15}$$

which is implicit when $c_0 \neq 0$ and which differs from the LF time-difference equation

$$z_{n+1} - 2z_n + z_{n-1} = (\Delta t)^2 a_n \tag{16}$$

by the effect of the force at different time levels.

The associated dispersion relation for the harmonic oscillator force $a = -z\omega_0^2$ with $z = \exp(-\mathrm{i}\omega\Delta t)$ is [7,8]

$$1/(\omega_0\Delta t)^2 + c_0 + c_1/z + c_2/z^2 + \ldots + z/(z-1)^2 = 0. \tag{17}$$

The RK schemes clearly do not belong the class (15) but can be made so by expressing a^*_{n+1} through the average $a_n = (a_{n-1} + a^*_{n+1})/2$. Eq. (3) then become

$$v_{n+1} - v_{n-1} = \frac{\Delta t}{2}(3a_n - a_{n-1}), \quad z_{n+1} - z_n = \Delta t\, v_n + \frac{\Delta t^2}{2}a_n \tag{18}$$

which corresponds to (15) with $c_0 = 0$, $c_1 = -1/2$, and $c_2 = c_3 = \cdots 0$. The associated dispersion relation

$$1/(\omega_0\Delta t)^2 + c_1/z + z/(z-1)^2 = 0 \tag{19}$$

has at least one unstable root $|z| > 1$ for $c_1 < 0$, so that the RK scheme is unconditionally unstable.

Let us now consider the SIMP method (13). Eq. (13) lead to

$$z_{n+1} - 2z_n + z_{n-1} = (\Delta t)^2(a_{n-1/2} + a_{n+1/2})/2. \tag{20}$$

To order $\mathrm{O}(\Delta t^4)$ this is just the leapfrog expression (16), stable in the interval $\omega_0\Delta t \leqslant 2$.

Finally, consider the semi-implicit form of the basic Euler method (henceforth denoted by SIEL)

$$v_{n+1} - v_n = \Delta t\, a_n, \quad z_{n+1} - z_n = \Delta t\, v_{n+1} \tag{21}$$

which is only 1st order accurate and clearly not time-centered. Nonetheless, Eq. (21) also lead to Eq. (16)! This indicates that the correspondence between the position time-difference equation (15) and the actual integration algorithm involving velocity is not unique. Clearly, the class (15) includes 1st order accurate schemes as a subset. Since the 1st order SIEL scheme (21) is so simple, it is useful to know that its stability properties are identical to those of the LF and the SIMP schemes.

We now verify the above results by the amplification matrix method of Hockney and Eastwood [9]. The present treatment clarifies in addition the role of the Jacobian matrix J. Any two-step integration scheme has the general form of a mapping of (v_n, z_n) onto (v_{n+1}, z_{n+1}):

$$v_{n+1} = f(v_n, z_n, v_{n+1}, z_{n+1}), \quad z_{n+1} = g(v_n, z_n, v_{n+1}, z_{n+1}). \tag{22}$$

Perturbations $(\varepsilon_v, \varepsilon_z)$ of the variables (v, z) are easily found to satisfy the equation

$$A\begin{pmatrix}\varepsilon_v\\ \varepsilon_z\end{pmatrix}_{n+1} = B\begin{pmatrix}\varepsilon_v\\ \varepsilon_z\end{pmatrix}_{n}, \quad A = \begin{pmatrix}1 - \partial f/\partial v_{n+1} & -\partial f/\partial z_{n+1}\\ -\partial g/\partial v_{n+1} & 1 - \partial g/\partial z_{n+1}\end{pmatrix}, \quad B = \begin{pmatrix}\partial f/\partial v_n & \partial f/\partial z_n\\ \partial g/\partial v_n & \partial g/\partial z_n\end{pmatrix} \tag{23}$$

which has the Jacobian matrix $(J) = A^{-1}B$. For an explicit scheme, the Jacobian equals det(B), for a semi-implicit scheme, the transformation (22) is easily manipulated into explicit form with modified f and g. If the eigenvalues λ of J lie within or on the unit circle of the complex plane, then perturbations do not grow in the integration process. This is the stability condition. The eigenvalues λ are obtained from the characteristic equation $\det(J - \lambda I) = 0$, i.e., from

$$\lambda^2 - \lambda(\partial f/\partial v + \partial g/\partial z) + \det(J) = 0. \tag{24}$$

Eq. (24) for the LF, the SIMP, and the 1st order SIEL schemes is

$$\lambda^2 - 2\lambda(1 + \Gamma) + 1 = 0 \tag{25}$$

while for the basic RK schemes (3) and (4) we have

$$\lambda^2 - 2\lambda(1 + \Gamma) + 1 + \Gamma^2 = 0. \tag{26}$$

The stability parameter Γ is defined in (6). The roots λ_1 and λ_2 of Eq. (24) satisfy $\lambda_1\lambda_2 = \det(J)$, so that the RK schemes are unstable. In the interval given by (6) the roots of (25) are complex-conjugate and therefore stable. Outside of the interval one of the roots is unstable.

For completeness we now give the accuracy of the above 2nd order schemes in terms of the magnitude of the lowest order (i.e., 3rd) truncation terms.

2.2. Accuracy-truncation errors

Let V and Z be the exact solutions of the equations of motion. On substitution of these into (2), (4), and (13), and expanding up to 3rd order in Δt, we obtain the following truncation error terms:

$$\delta_z^{\mathrm{LF}} = \frac{1}{24}\dot{a}(\Delta t)^3, \quad \delta_v^{\mathrm{LF}} = -\frac{1}{24}\ddot{a}(\Delta t)^3, \tag{27a}$$

$$\delta_z^{\mathrm{SIMP}} = \frac{1}{12}\dot{a}(\Delta t)^3, \quad \delta_v^{\mathrm{SIMP}} = \frac{1}{24}\ddot{a}(\Delta t)^3, \tag{27b}$$

$$\delta_z^{\mathrm{RK}} = -\frac{1}{6}\dot{a}(\Delta t)^3, \quad \delta_v^{\mathrm{RK}} = \frac{1}{12}\ddot{a}(\Delta t)^3, \tag{27c}$$

where $\dot{a} = \mathrm{d}a/\mathrm{d}t$. Hence if $a = a(z)$, then $\dot{a} = v(\mathrm{d}a/\mathrm{d}z)$. The LF scheme is the most accurate of the three, closely followed by the SIMP scheme.

3. Calculation of orbits in a plane wave and nonlinear stability

In order to illustrate the practical performance of the schemes discussed above we now compute charged particle trajectories in a non-linear propagating wave, i.e., we solve the equation

$$\dot{v} = \omega v_q \sin(\omega t - kz), \quad \dot{z} = v. \tag{28}$$

Here $v_q = eE_0/m\omega$ is the quiver velocity and E_0 is the applied electric field strength. For our purposes it is convenient that a first integral exists in the wave frame of reference. This permits an easy check on the stability of the integration process which is here related to the onset of intrinsic stochasticity. Below the stochasticity threshold, the trapped particle orbits from the area-preserving LF and SIMP integration schemes exhibit outstanding long-term stability owing to the existence of an invariant of the iterated difference equations [11].

The LF velocity vector is shifted back in time by half a time step with respect to the position vector. Just as the LF velocities and positions have to be aligned for the calculation of kinetic and potential energies [8], such alignment is necessary for the construction of LF phase-space orbits. We therefore use an aligned LF velocity equal to the average between two successive velocity time levels. Auerbach and Friedman [11] use the term "isochronous leapfrog" for this version of LF and discuss a number of its convenient properties.

We work in normalized variables such that

$$\tau = \omega t, \quad \zeta = kz, \quad u = vk/\omega, \quad \mathrm{d}u/\mathrm{d}\tau = Y^2 \sin(\tau - \zeta), \tag{29}$$

where $\omega_B^2 = k\omega v_q$ is the bounce frequency and $Y = \omega_B/\omega$. With the transformation

$$\zeta' = \zeta - \tau, \quad u' = u - 1 \tag{30}$$

the explicit time dependence is removed from (28) and the first integral is

$$u'^2 = u_0'^2 + 2Y^2(\cos\zeta' - \cos\zeta_0'). \tag{31}$$

When u'^2 is negative in some range of ζ' then the electron is trapped on a closed orbit within the separatrix, given by $u'^2 = 2Y^2(1 + \cos\zeta')$. Ideally, the particle will trace the trapped orbit indefinitely, but loss of accuracy and stability of the integration process will lead to departures from the exact orbit (31). To select a particular trapped orbit relatively close to the separatrix we set the initial condition to $\zeta_0' = 0$ at the stable elliptic point and $u_0' = 1.5Y$.

How stability is here related to intrinsic stochasticity is easily seen from the semi-implicit Euler SIEL scheme (21), which in the normalized variables (29), (30) reads

$$u_{n+1}' - u_n' = -\Delta\tau\, Y^2 \sin(\zeta_n'), \quad \zeta_{n+1}' - \zeta_n' = \Delta\tau\, u_{n+1}' \tag{32}$$

Multiplying through by $\Delta\tau$ immediately gives the standard map [12]

$$I_{n+1} - I_n = -K\sin(\Phi_n), \quad \Phi_{n+1} - \Phi_n = I_{n+1}, \tag{33}$$

where $I = u'\Delta\tau$ is a normalized action, $\Phi = \zeta'$ is the angle variable, and $K = (\Delta\tau\, Y)^2$ is the stochasticity parameter. Stochasticity onset occurs around $K = 1$ [12], i.e., around $\omega_B\Delta t = 1$. The isochronous leapfrog method leads to a symmetrized time-centered version of (33) [10] and clearly has the same stochasticity threshold $K = 1$.

The SIMP scheme (13) likewise leads to a standard map. With the same normalization as above Eqs. (13) become

$$I_{n+1} - I_n = -K\sin(\Phi_n + I_n/2), \quad \Phi_{n+1} - \Phi_n = (I_n + I_{n+1})/2 \tag{34}$$

so that with the new angle $\Omega = \Phi + I/2$ we immediately obtain

$$I_{n+1} - I_n = -K\sin(\Omega_n), \quad \Omega_{n+1} - \Omega_n = I_{n+1}. \tag{35}$$

The difference between the LF and SIMP standard maps is that the LF action period is 2π whereas the SIMP action period is 4π, as is clear from (33) and (34). The action period equals the distance between period 1 fixed points, i.e., between the primary islands of the mapping [12]. We also note that the semi-implicit Euler scheme (21) has the same linear and nonlinear stability properties as the LF and SIMP schemes. This goes to show

that a simple 1st order scheme can posses the same or better linear and nonlinear stability properties than more accurate higher-order integration algorithms.

We now present some integration results as a function of the stochasticity parameter K. We will compare LF and SIMP orbits with the exact orbit (31) and with orbits from the basic 2nd and 4th order RK schemes. We compute the orbits in the fixed reference frame (u,ζ) and then transform them to the wave frame (u',ζ') using (30).

For the first series of figures, Figs. 1–5, we compute trapped particle orbits for about 500 cycles. The reference exact orbits (31) are labeled EX, the LF orbits are labeled LF, the SIMP orbits (13) are labeled SIMP, the SIEL orbits from (21) are labeled SIEL, and orbits from RK methods are labeled RK2 or RK4, respectively. The separatrix is evident as the finer line. Fig. 1 shows the exact orbit (31), and the 2nd order RK and SIEL orbits from, respectively, Eqs. (4) and (21), for weak non-linearity $K = 0.05$. The 2nd order RK result has already collapsed, and the 1st order SIEL orbit is already deformed. With increasing K the deformation of SIEL orbits increases, but the orbits remain stable up to the limit $K = 1$. In Figs. 2 and 3 we show the exact,

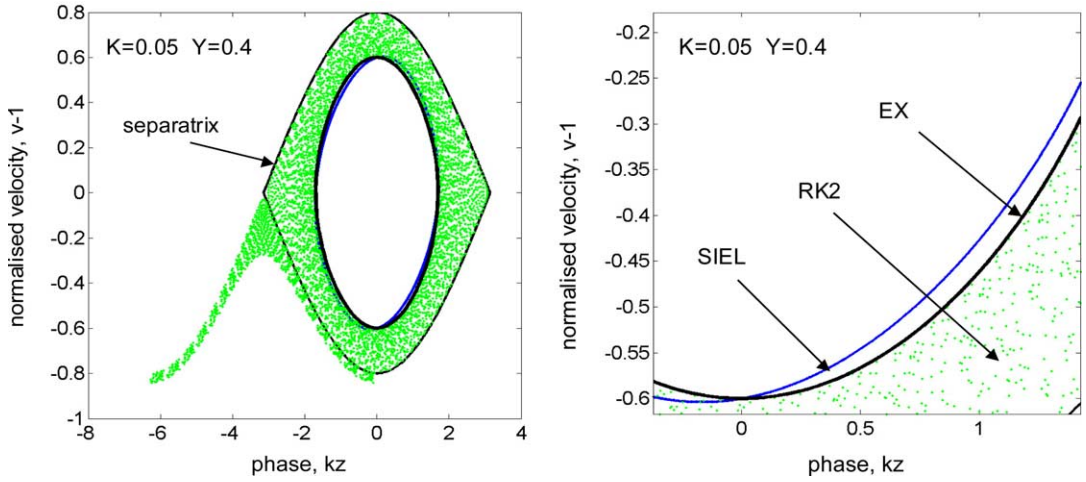

Fig. 1. (left panel) The separatrix and trapped particle orbits in the wave frame of (28) for $K = (\Delta t\omega)^2 = 0.05$. Exact orbit from (31), SIEL orbit from (21), 2nd order RK orbit from (3). (right panel) Zoom.

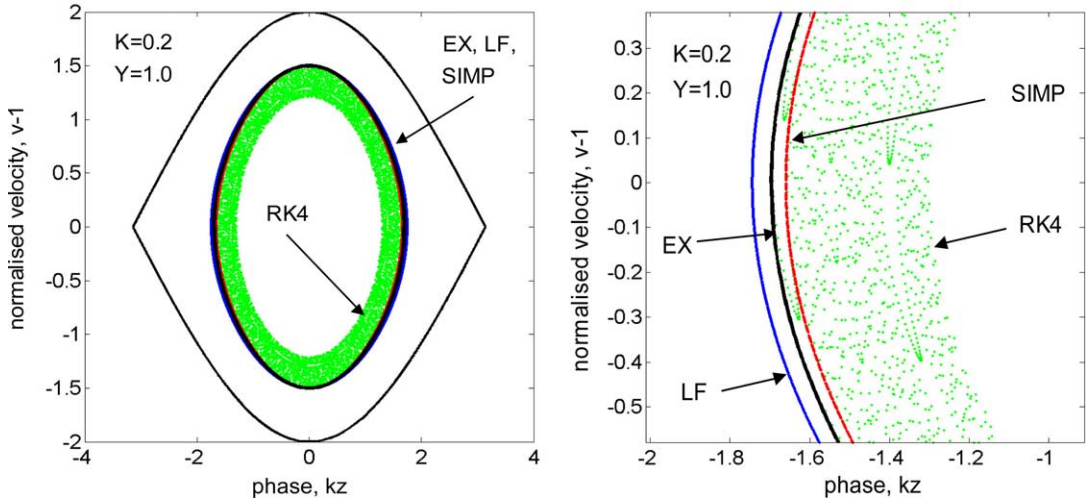

Fig. 2. (left panel) The separatrix, exact orbit, LF orbit, SIMP orbit, and orbit from the 4th order RK method, for $K = 0.2$. (right panel) Zoom.

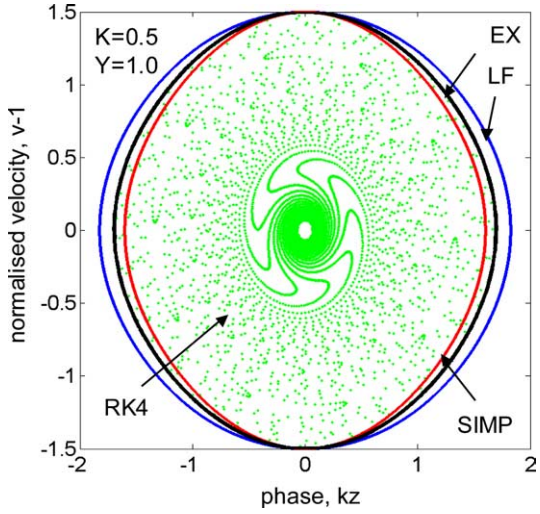

Fig. 3. Exact orbit, LF orbit, SIMP orbit, and orbit from the 4th order RK method, for $K = 0.5,\ Y = 1$.

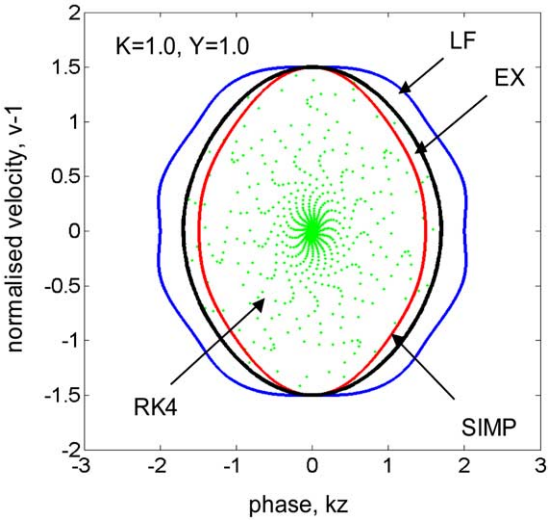

Fig. 4. Exact orbit, LF orbit, SIMP orbit, and orbit from the 4th order RK method, for $K = 1,\ Y = 1$.

LF, SIMP, and 4th order RK orbits for $K = 0.2$ and $K = 0.5$. The 4th order RK method [4] is not area preserving and clearly possesses negative eigenvalues. Figs. 4 and 5 then indicate the collapse of the LF orbit at the stability limit and beyond. Curiously, the SIMP orbit appears more resilient. The collapse of the 2nd and 4th order orbits observed in Figs. 1–5, even as early as for $K = 0.05$ in Fig. 1, emphasizes the importance of using an area-preserving integration scheme for integrable Hamiltonian systems.

Complementing the single orbit calculations of Figs. 1–5 are the Poincare surface of section plots of Figs. 6 and 7, action versus phase mod 2π. The phase is shifted by $-\pi$ in order to center the primary islands. In each surface of section we launched 50 particles with action initially uniformly randomly distributed in the interval $(0, 4\pi)$. The difference between the leapfrog and SIMP originates from a different periodicity of the action in these mappings. The figures confirm what be seen from (33) and (34), namely that the LF action period is 2π while the SIMP action period is 4π. Thus, in the LF case the primary islands are seen in the figures to be separated by 2π, whereas in the SIMP case they are separated by 4π. The SIMP and LF surfaces of section in Fig. 7 nicely indicate the appearance of secondary islands half-way between the primary islands.

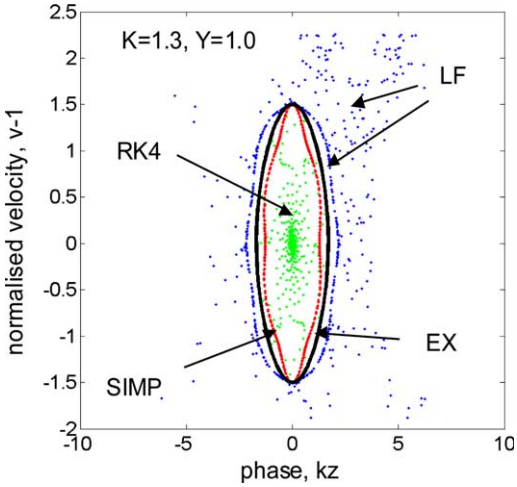

Fig. 5. Exact orbit, LF orbit, SIMP orbit, and orbit from the 4th order RK method, for $K = 1.3$, $Y = 1$.

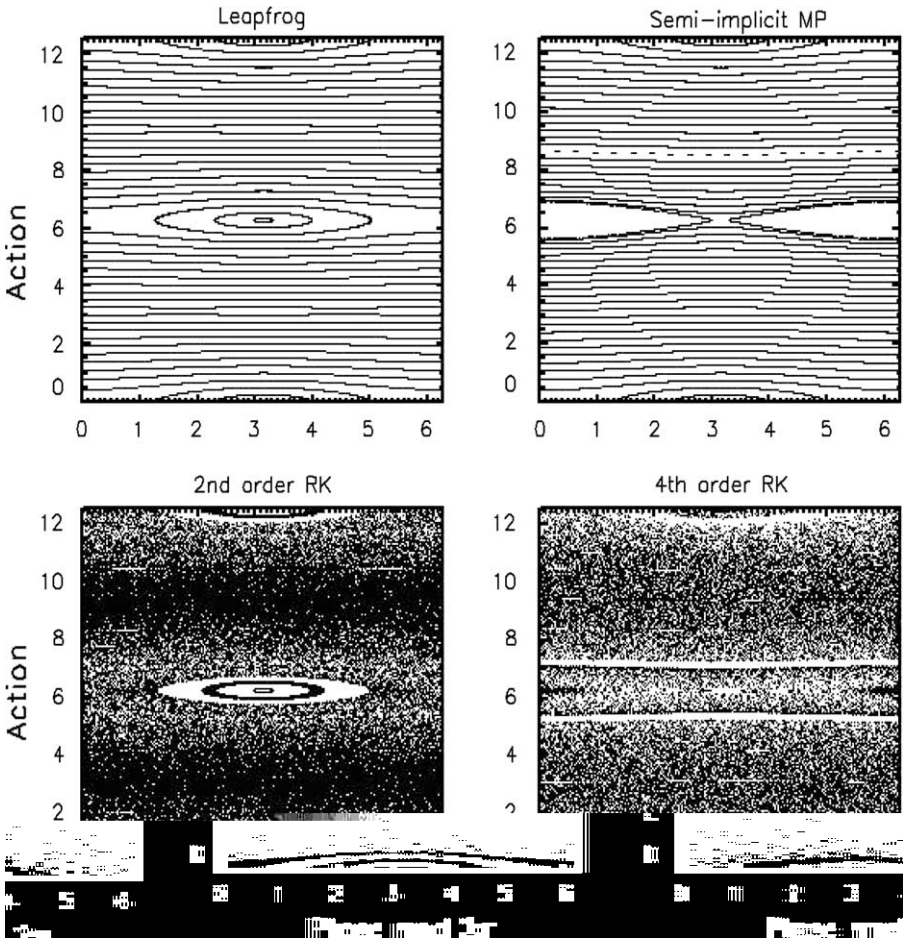

Fig. 6. Poincaré surface of section plots, normalized action versus (phase-π) mod 2π, from LF, SIMP, 2nd order RK, and 4th order RK integration schemes for Eq. (28). $K = 0.1$.

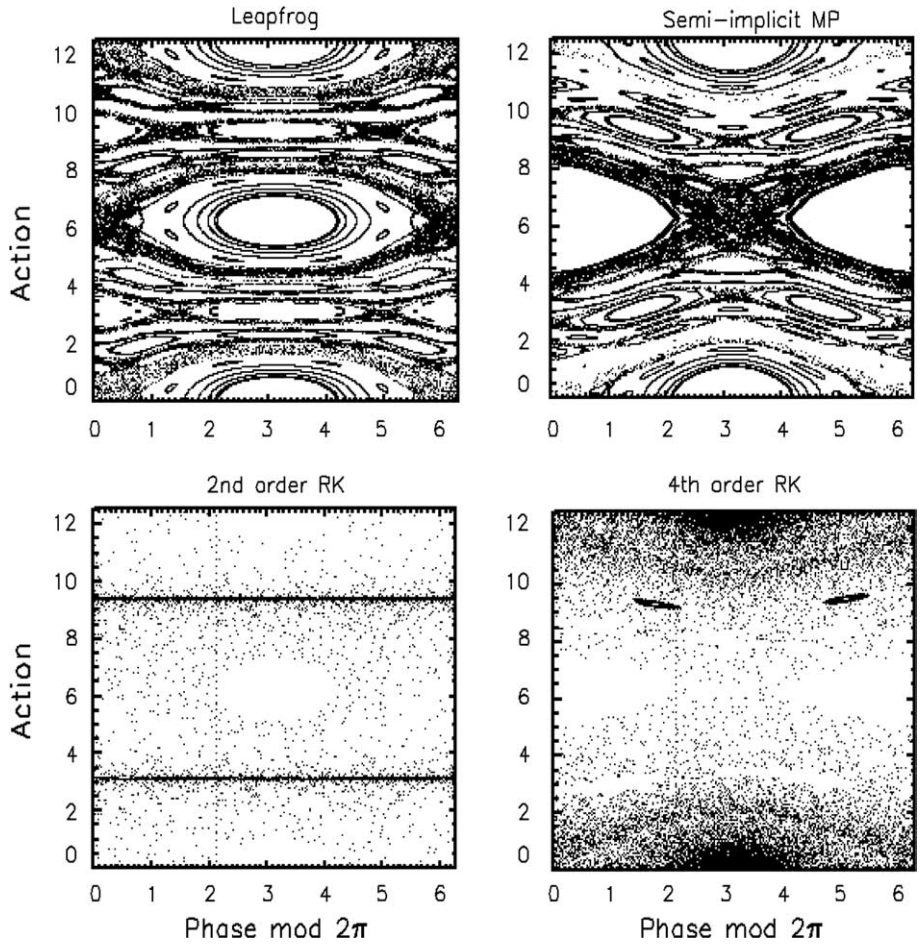

Fig. 7. Poincaré surface of section plots, normalized action versus (phase-π) mod 2π, from LF, SIMP, 2nd order RK, and 4th order RK integration schemes for Eq. (28). $K = 1.0$.

Already early on for $K = 0.1$ we note in Fig. 6 that orbits from the non-area-preserving RK schemes have collapsed near and outside of the separatrix, while the LF and SIMP orbits remain regular. At the stability limit $K = 1$ in Fig. 7 the RK cases are almost globally stochastic, while stochasticity in the LF and SIMP cases is just starting to develop around and outside the separatices.

4. Particle orbits for velocity-dependent forces

4.1. Calculations of particle orbits in a static magnetic field

Consider the equations of motion of a charged particle in a static magnetic field oriented along the z-axis of a Cartesian coordinate system $\vec{r} = (x, y, z)$:

$$\frac{\mathrm{d}v_x}{\mathrm{d}t} = \omega v_y, \quad \frac{\mathrm{d}v_y}{\mathrm{d}t} = -\omega v_x, \quad \frac{\mathrm{d}v_z}{\mathrm{d}t} = 0, \quad \frac{\mathrm{d}\vec{r}}{\mathrm{d}t} = \vec{v}. \tag{36}$$

The system (36) is four-dimensional since the z-direction separates out and plays no role. Kinetic energy is conserved so we can compare numerical integration results with the reference gyro-orbit invariants

$$v_x^2 + v_y^2 \equiv v_0^2, \tag{37a}$$

$$[v_{x0} + \omega(y - y_0)]^2 + [v_{y0} - \omega(x - x_0)]^2 = v_0^2. \tag{37b}$$

We will present results from four different area-preserving integration schemes: Boris' scheme [8,14], SIMP, and two different leapfrog schemes: implicit and semi-implicit. The system (36) is interesting since the higher dimensionality allows more than one implementation of the LF and SIMP schemes. We also note that velocity space of system (36) forms a self-contained subspace of phase-space and describes, in fact, the harmonic oscillator, which is therefore automatically included here as a special case. For semi-implicit LF and SIMP the linear stability criterion $\omega\Delta t < 2$, discussed in Section 3, applies, but for implicit LF there is no restriction on $\omega\Delta t$ [10]. We note in advance that the velocity space results from all these schemes appear acceptable; the velocity-space gyro-orbit form Boris' method is of course exact. Substantial differences between some results however appear in configuration space.

The computations are performed in normalized variables τ, u and ρ, such that $\tau = t\omega$, $\vec{v} = v_T\vec{u}$, $\vec{r} = r_L\vec{\rho}$, where $\omega = eB_z/m$ is the cyclotron frequency, v_T is the thermal velocity, $r_L = v_T/\omega$ is the Larmor radius, and $\vec{\rho} \equiv (\xi, \eta, \zeta)$. Eqs. (36) thus become

$$\frac{du_x}{d\tau} = u_y, \quad \frac{du_y}{d\tau} = -u_x, \quad \frac{du_z}{d\tau} = 0, \quad \frac{d\vec{\rho}}{d\tau} = \vec{u}. \tag{38}$$

The implicit LF scheme uses $u_n = (u_{n+1/2} + u_{n-1/2})/2$ on the right-hand side of the first two equations in (38) and the centered velocities in the position equations. Specifically,

$$\begin{pmatrix} u_x \\ u_y \end{pmatrix}_{n+1/2} = (J_U)\begin{pmatrix} u_x \\ u_y \end{pmatrix}$$

q u J E F f

From a computational point of view an important distinction between the semi-implicit SILF and SIMP schemes (41) and (44) and the implicit LF scheme (39) are the respective dispersion relations. For the implicit scheme with $\alpha = \Delta\tau/2$ we have $\alpha = \tan(\alpha)$, which always has a solution [10], whereas in the SILF and SIMP cases $\alpha = \sin(\alpha)$, which gives the well-known stability limit $\alpha < 1$.

We also show results from the Boris integration scheme for particle motion in a static magnetic field [8,14] applied to system (36). We note in this context that the invariant (37a) is reproduced exactly by that method, since the velocity gyro-motion is resolved exactly:

$$u_x(\tau) = u_{x0}\cos\tau + u_{y0}\sin\tau, \quad u_y(\tau) = -u_{x0}\sin\tau + u_{y0}\cos\tau. \tag{45}$$

Two different time sequences of velocity are necessary here. First, starting at $\tau = 0$ gives the time-aligned velocity orbit for comparison with orbits from other schemes. Second, for the centered calculation of positions, the velocities are determined at half time intervals by an initial backward shift through a half rotation $-\tau/2$.

We now discuss some of the numerical results, keeping in mind that the velocity gyro-orbit also represents the harmonic oscillator. Well below stability threshold $\Delta\tau \ll 2$ the 2nd order RK orbit from Eq. (3) already starts spreading out because of area non-preservation. In contrast, the velocity space orbits from the area-preserving LF, SILF, SIMP and Boris schemes practically overlap and agree with the exact orbit (37a). Some of the sub-threshold results are illustrated in Fig. 8 where we show the exact, SIMP, and 2nd order RK velocity and configuration space orbits for $\Delta\tau = 0.15$. The initial conditions for the calculations of Figs. 8–10 are $u_{x0} = u_{y0} = 1$, $\xi_0 = \eta_0 = 0$.

As stability threshold $\Delta\tau = 2$ is approached the LF, SILF and SIMP schemes still produce good velocity space gyro-orbits, but the corresponding configuration space gyro-orbits start disagreeing with each other and with the exact orbit calculated from $d\vec{r}/dt = \vec{v}$. This is shown in Figs. 9(a) and (b) where we compare results from SILF and SIMP schemes, from respectively (41) and (44), with the respective exact orbits (37a), (37b) at near threshold conditions $\Delta\tau = 1$.

Completing this picture is Fig. 10 where for the same near-threshold conditions $\Delta\tau = 1$, we compare results from the LF, SIMP and Boris' schemes with the respective exact orbits (37a), (37b). The Boris orbit is labeled B. Figs. 9(a) and 10(a) attest to the area-preserving property and outstanding stability of the SIMP scheme in this particular example of linear oscillations in velocity space. On the other hand, Figs. 9(b) and 10(b) show a substantial departure of the LF and SIMP spatial gyro-orbits from the exact orbit (37b). More work is needed

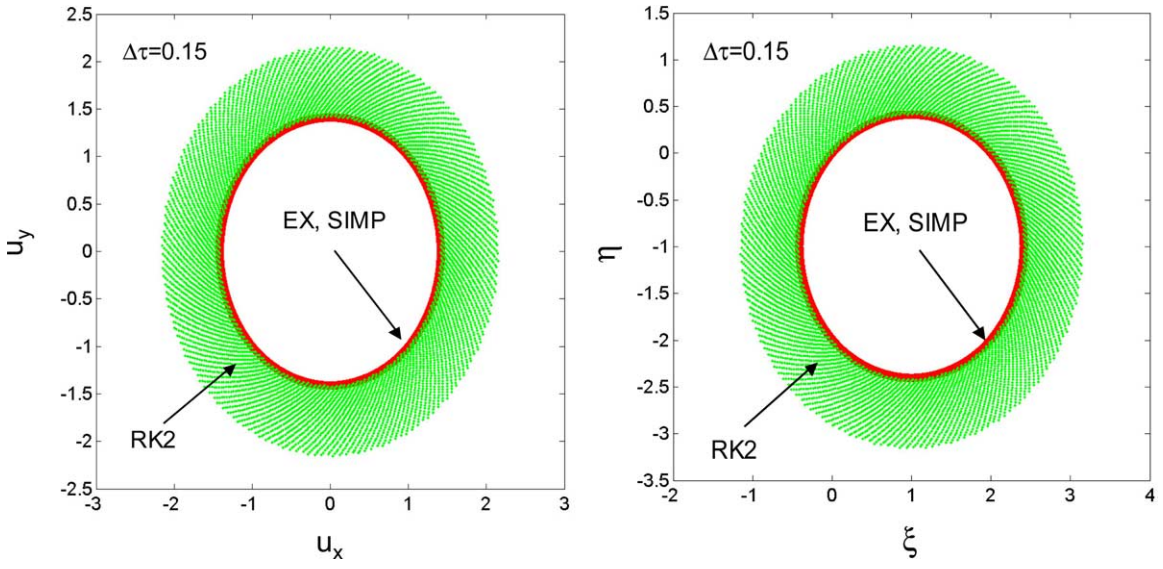

Fig. 8. The exact, SIMP, and 2nd order RK gyro-orbits for $\omega\Delta t = 0.15$. (left panel) Velocity space results, (right panel) configuration space results.

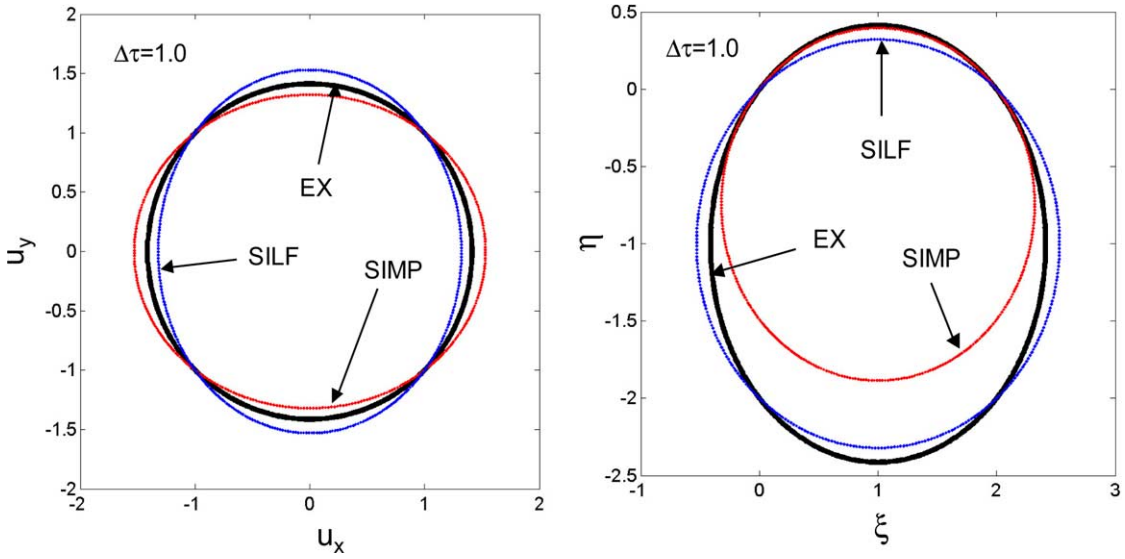

Fig. 9. The exact, SILF and SIMP gyro-orbits for $\omega\Delta t = 1$. (left panel) Velocity space results, (right panel) configuration space results.

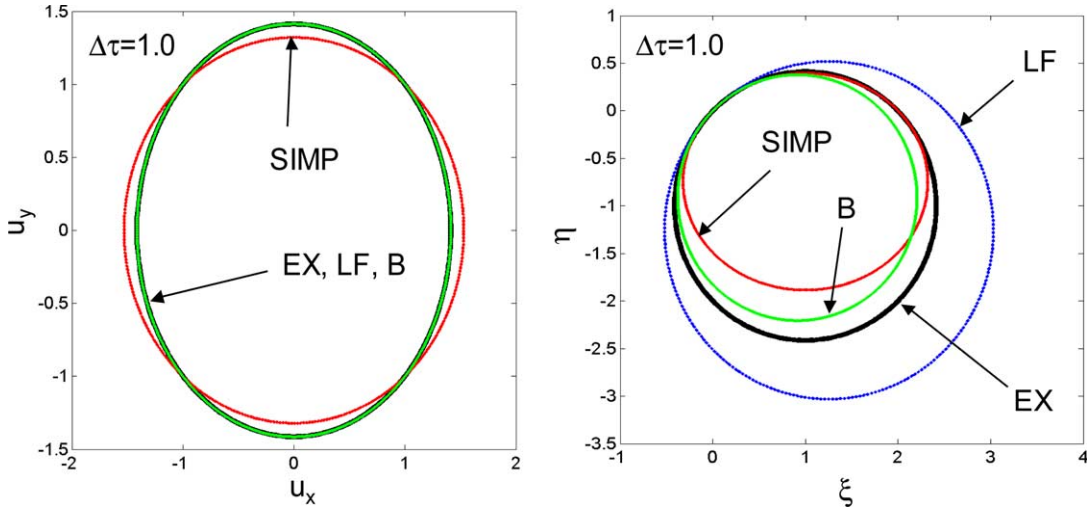

Fig. 10. The exact, LF, SIMP, and Boris gyro-orbits for $\omega\Delta t = 1$. (left panel) Velocity space results (the exact, LF and Boris orbits overlap), (right panel) configuration space results.

to understand the observed differences in configuration space when more than two dimensions of phase space are involved.

4.2. Particle orbits in the presence of nonlinear dissipation

In order to demonstrate the performance of the SIMP method in a non-linear case of a velocity-dependent force, we consider the model problem of a harmonic oscillator perturbed by a non-linear dissipative term, in normalized variables τ, u, ζ such that with $\tau = \omega t$ we have

$$\mathrm{d}u/\mathrm{d}\tau = \mu(1-\zeta^2)u^m - \zeta, \quad \mathrm{d}\zeta/\mathrm{d}\tau = u. \tag{46}$$

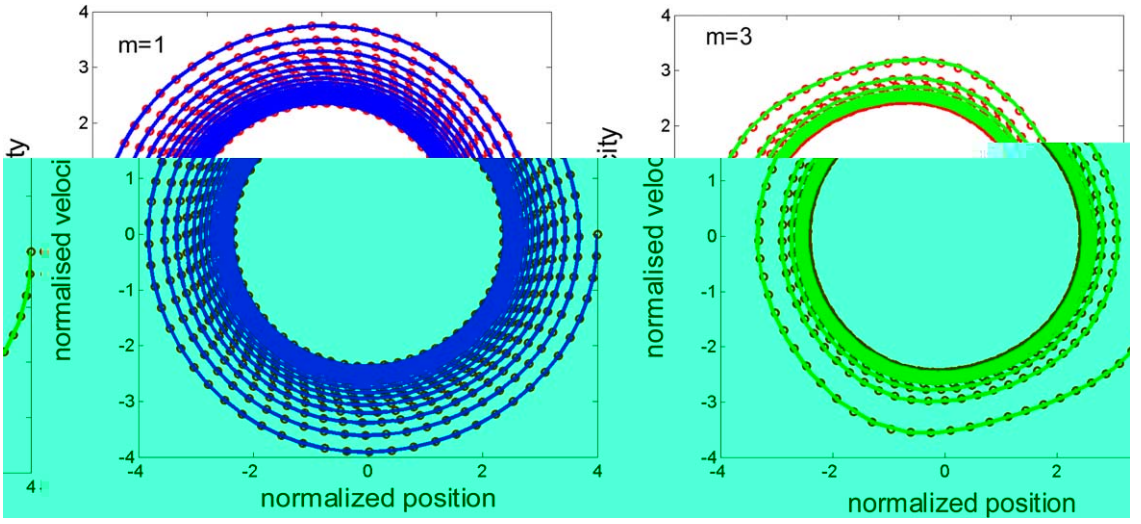

Fig. 11. Numerical solutions of Eq. (46) for $\Delta\tau = 0.1$ and $\mu = 0.01$. The solution from SIMP is marked by dots, the solutions from LF and the 4–5th order RK method are marked by a line. (left panel) van der Pol equation $m = 1$, the limit cycle is the circle $\rho = 2$, (right panel) $m = 3$.

We consider two cases of the exponent m: $m = 1$ and $m = 3$. In both cases the asymptotic solution is a stable limit cycle, i.e., a closed orbit whose radius only depends on m and on the perturbation parameter μ. The equation thus describes a stable oscillatory system independent of the initial state. For $m = 1$ Eq. (46) describes the van der Pol oscillator which for small $\mu \ll 1$ tends to a stable limit cycle of radius $\rho = \sqrt{u^2 + \zeta^2} \cong 2$ [13]. The $m = 1$ case has a simple LF implicit solution which is shown together with the SIMP solution and the limit cycle in Fig. 10(a). For $m = 3$, the non-linearity is stronger, the asymptotic solution is still a limit cycle, and an LF implicit solution is no longer easy to implement so that in Fig. 10(b) we compare the SIMP solution with the solution from the explicit 4–5th order RK method of [15].

In the $m = 1$ van der Pol case of Fig. 11(a), the SIMP and LF orbits agree with each other very nicely and wind up onto the predicted limit cycle $\rho = 2$. In the strongly non-linear case $m = 3$ of Fig. 11(b), we observe the SIMP solution tracking the more accurate 4–5th order RK solution towards a common limit cycle quite faithfully. The calculations of Fig. 11 were done with a time step $\Delta\tau = 0.1$ and a perturbation parameter $\mu = 0.01$.

5. Conclusion

An integration scheme for particle equations of motion in a PIC code should ideally be simple, accurate and not unconditionally unstable. Simplicity is required owing to the large number of particles in such codes, while accuracy and stability are essential when the equations are advanced for many time steps. Accuracy has to do with truncation errors and stability with the evolution of perturbations of the exact solution. A compromise between simplicity and accuracy leads to the choice of 2nd order accurate schemes. One such scheme which satisfies the above criteria is the well known leapfrog method, implicit for forces dependent on velocity. With the exception of a few simple cases (e.g., Lorentz force, linear damping) an implicit treatment is computationally very demanding, time consuming and possibly prohibitive altogether. Where easily applicable, the leapfrog method has become, because of its desirable properties enumerated above, a standard for assessing the properties and performance of other candidate integration schemes for the equations of motion for PIC codes [6,7]. A more recent Hamiltonian treatment of the leapfrog method applied to nonlinear oscillations [10,11] has revealed "numerical stochasticity" [10], i.e., stochasticity arising from the time differencing, as the principal limiting factor in the integration process of non-linear periodic systems. Hand-in-hand with the study of numerical stochasticity, the process of long-term phase error accumulation was analyzed and the existence of a

constant of motion in the discrete integration process was recognized as being responsible for the long term survival of closed particle orbits [11].

In this context we have set here out to develop and test a more generally applicable explicit alternative to the LF method. In this endeavor we concentrated on the 2nd order Runge–Kutta schemes. At the outset their attraction is simplicity and approximate time-centering. However, unlike the usual leapfrog scheme for velocity independent forces, the standard 2nd (as well as 4th) order RK schemes presented in the literature [4,5] do not preserve phase space measure and are numerically unconditionally unstable. In order to understand why such schemes are in principle objectionable, it is useful to realize that the time differencing constitutes a perturbation of the system Hamiltonian and view the time differencing as a mapping of phase space onto itself. The mapping produces phase space flow constrained by the perturbed Hamiltonian and should therefore be area preserving [12]. Led by this principle, we constructed the area-preserving combination (13) of the basic 2nd order schemes (3) and (4) and demonstrated its outstanding qualities in the examples of Sections 3 and 4. The procedure we recommend for securing area-preservation is given in Sections 2.1 and 4.1: implement the time differencing of as many phase space variables as possible semi-implicitly, i.e., using variables of the next time step already calculated on the given time step. At least one variable has to be of course advanced explicitly and this is done using the midpoint force as is Eqs. (13).

We have shown that the new integration scheme SIMP (semi-implicit midpoint), Eq. (13), shares identical linear and non-linear stability properties with the leapfrog scheme. For forces independent of velocity both the LF and SIMP schemes require only one evaluation of the force per time step. For forces dependent on velocity, the LF scheme becomes implicit, whereas the SIMP scheme remains semi-implicit and requires two evaluations of the force per time step.

Another problem of general interest is the numerical stability of an integration scheme in wave–particle interactions. This involves extending the well-known linear oscillator stability condition $\Delta t\,\omega_0 < 2$ to nonlinear oscillations driven by a periodic force. Friedman and Auerbach [10] have previously established that numerical stability for nonlinear periodic systems is related to intrinsic stochasticity induced by the time differencing. In this respect it is helpful that for a plane wave the leapfrog scheme (2) as well as the new SIMP scheme (13) can be written in form of the standard map. This then immediately leads to the integration stability condition $\Delta t\,\omega_B < 1$, where ω_B is the particle bounce frequency.

This work was motivated by the need to develop a suitable integration method for a quasi-neutral PIC code for application to tokamak edge problems. In a quasi-neutral PIC code the self-consistent field is determined not from the Poisson equation but rather from the fluid electron momentum equation [16], so that the self-consistent force depends on the electron pressure gradient. Other velocity-dependent forces in PIC simulations which prohibit the use of the leapfrog method are, e.g., external Langevin processes which can describe particle collisions and/or radio-frequency plasma heating. Our work on the development and application of a quasi-neutral PIC code to tokamak plasma edge problems will be presented elsewhere [17].

Note added in proof

In regard to the area preservation property of maps used herein, we thank Dr Dominique Escande for pointing out to us during a recent discussion the more general nature of symplectic maps relevant in more than two dimensions, and therefore applicable in the four dimensional case of Section 4.1.

Acknowledgments

We thank Dr. R. Dejarnac and Dr. R. Pánek for reading the manuscript and useful discussions, and our colleagues and the staff at IPP-Prague and DRFC, Cadarache, for their support and encouragement in the course of this work.

References

[1] O. Buneman, J. Comput. Phys. 1 (1967) 517.
[2] W.M. Manheimer, M. Lampe, G. Joyce, J. Comput. Phys. 138 (1997) 563.

[3] V. Fuchs, J.P. Gunn, M. Goniche, V. Petržílka, Nucl. Fusion 43 (2003) 341.
[4] M. Abramowitz, I.A. Stegun, Handbook of Mathematical Functions, National Bureau of Standards Applied Mathematics Series, vol. 55, Washington, DC, 1964 (Chapter 25).
[5] W.H. Press, S.A. Teukolsky, W.T. Vetterling, B.P. Flannery, Numerical Recipes in Fortran 77, Cambridge University Press, Cambridge, 1992 (Chapter 16).
[6] A.B. Langdon, J. Comput. Phys. 30 (1979) 202.
[7] B.I. Cohen, A.B. Langdon, A. Friedman, J. Comput. Phys. 46 (1982) 15.
[8] C.K. Birdsall, A.B. Langdon, Plasma Physics via Computer Simulation, Hilger, Bristol, 1991.
[9] R.W. Hockney, J.W. Eastwood, Computer Simulation using Particles, Hilger, Bristol, 1988.
[10] A. Friedman, S.P. Auerbach, J. Comput. Phys. 93 (1991) 171.
[11] S.P. Auerbach, A. Friedman, J. Comput. Phys. 93 (1991) 189.
[12] A.J. Lichtenberg, M.A. Lieberman, Regular and Stochastic Motion, Springer, New York, 1983.
[13] N. Minorsky, Nonlinear Oscillations, Van Nostrand Company, Inc., Princeton, NJ, 1962 (Chapters 3 and 9).
[14] J.P. Boris, Relativistic plasma simulation – optimisation of a hybrid code, in: Proceedings of the Fourth Conf. Numerical Sim. Plasmas, Naval Research Lab., Washington, DC, 2–3 November, 1970, pp. 3–37.
[15] J.R. Dormand, P.J. Prince, J. Comput. Appl. Math. 6 (1980) 19.
[16] G. Joyce, M. Lampe, S.P. Slinker, W. Manheimer, J. Comput. Phys. 138 (1997) 540.
[17] J.P. Gunn, C. Boucher, M. Dionne, et al., Plasma edge physics in an actively cooled tokamak, invited talk to be presented at the International Conference Plasma 2005 on Research and Applications of Plasmas, September 6–9, Opole, Poland, 2005.